Estuaries and Coasts Vol. 29, No. 4, p. 653–664 August 2006

Tidally-induced Shear Stress Variability above Intertidal Mudflats in the Macrotidal Seine Estuary

R. VERNEY[1,2], J.-C. BRUN-COTTAN[3], R. LAFITE[1], J. DELOFFRE[1], and J. A. TAYLOR[4]

[1] *UMR CNRS 6143 Morphodynamique Continentale et Côtière, University of Rouen, M2C, 76821 Mont Saint Aignan Cedex, France*
[2] *Institut Français de Recherche pour l'Exploitation de la Mer (IFREMER) DYNECO-PHYSED, BP70, 29280 Plouzane, France*
[3] *UMR CNRS 6143 Morphodynamique Continentale et Côtière, University of Caen, M2C, 24 Allée des Tilleuls, 14000 Caen, France*
[4] *Coastal and Estuarine Research Group, School of Life Sciences, University of Sussex, Falmer, Brighton, BN1 9QJ, U.K.*

ABSTRACT: Tidal currents and the spatial variability of tidally-induced shear stress were studied during a tidal cycle on four intertidal mudflats from the fluvial to the marine part of the Seine estuary. Measurements were carried out during low water discharge (<400 $m^3 s^{-1}$) in neap and spring tide conditions. Turbulent kinetic energy, covariance, and logarithmic profile methods were used and compared for the determination of shear stress. The c_{TKE} coefficient value of 0.19 cited in the literature was confirmed. Shear stress values were shown to decrease above mudflats from the mouth to the fluvial part of the estuary due to dissipation of the tidal energy, from 1 to 0.2 N m^{-2} for spring tides and 0.8 to 0.05 N m^{-2} for neap tides. Flood currents dominate tidally-induced shear stress in the marine and lower fluvial estuary during neap and spring tides and in the upper fluvial part during spring tides. Ebb currents control tidally-induced shear stress in the upper fluvial part of the estuary during neap tides. These results revealed a linear relationship between friction velocities and current velocities. Bed roughness length values were calculated from the empirical relationship given by Mitchener and Torfs (1996) for each site; these values are in agreement with the modes of the sediment particle-size distribution. The influence of tidal currents on the mudflat dynamics of the Seine estuary was examined by comparing the tidally-induced bed shear stress and the critical erosion shear stress estimated from bed sediment properties. Bed sediment resuspension induced by tidal currents was shown to occur only in the lower part of the estuary.

Introduction

Over the past 20 yr, various studies have described how macrotidal estuarine systems vary with time and in space (Uncles et al. 1998; Dyer et al. 2000; Le Hir et al. 2000). Among all physical, chemical, and biological gradients observed in estuaries, the hydrodynamic parameters are considered to be the most important forcing parameter for all microscale and macroscale estuarine processes (Mikes et al. 2004). Hydrodynamic parameters are controlled by the seasonal fluvial discharge, tidal propagation, and episodic energetic events such as swell and wind-induced and vessel-induced waves. Other studies extended our knowledge on hydrodynamic forcing parameters in estuaries and their effect on sediment dynamics such as turbidity maximum dynamics (Uncles et al. 1998, 2002; Brenon and Le Hir 1999; Dyer et al. 2004) and mudflat dynamics (Dyer et al. 2000; Le Hir et al. 2000). Whatever the system studied, estuarine sediments entail a variety of mechanisms in a complex cycle (Eisma 1993): erosion, resuspension, flocculation, settling, deposition, and consolidation. Erosion and resuspension of bed sediments occur when the bottom shear stress reaches critical values (Mitchener and Torfs 1996; Black 1998). This threshold value is described in the literature as a function of bed sediment properties such as mud-sand composition, compaction, bed roughness length, and biological benthic activity (Mitchener and Torfs 1996; Maa et al. 1998; Tolhurst et al. 2000; Droppo et al. 2001; Sanford and Maa 2001). Once the shear stress exceeds a critical value, bed sediments are eroded and resuspended in the water column and are subjected to flocculation processes and horizontal transport. Similarly to erosion and resuspension processes, flocculation processes, described as the aggregation and fragmentation of cohesive particles (van Leussen 1994; Eisma 1996), are driven by sediment properties and biological activity but predominantly by the turbulence variability (Manning and Dyer 1999; Mikes et al. 2004). In our case, suspended particles are eventually transported out of the system by the river flow and tidal flow or they settle, depending on particle

* Corresponding author; tele: +33 (0)2 98 22 40 40; fax: +33 (0) 2 98 22 48 64; e-mail: romaric.verney@ifremer.fr

characteristics, such as size and density (Dyer 1994; Manning and Dyer 1999), and turbulence in the water column.

All of these studies revealed the key role played by hydrodynamic forcing parameters on sediment transport processes in estuaries. According to the morphological conceptual model described by Dalrymple et al. (1992), hydrodynamic forcing and the resulting intensity of shear stress vary in a macrotidal estuary between the mouth and the tidal limit. This conceptual model proposes dividing an estuary according to the morphological and hydrodynamic features of each section. In the case of macrotidal estuaries, the model proposes dividing the estuary into three compartments: river dominated, intermediate-mixed energy, and marine dominated compartments.

Previous studies on in situ turbulence measurements in estuaries focused on single point measurements, mainly on mudflats at the mouth or near the turbidity maximum zone (Fugate and Friedrichs 2002; Nikora et al. 2002; Dyer et al. 2004). These studies examined the influence of hydrodynamic forcing parameters on local sediment dynamics, but did not explain the spatial variability of the bottom shear stress within an estuary and particularly its effect on dynamics in areas where fine sediments accumulate. The purpose of this study was to make high-frequency near-bed turbulence measurements on fine sedimentation areas representative of the different morphodynamic and hydrodynamic parts of the macrotidal Seine estuary during low water discharge and during both neap and spring conditions. The objective of the study was to investigate tidally-induced shear stress variations in the Seine estuary and to provide shear stress ranges for each estuarine compartment of the conceptual model of Dalrymple et al. (1992).

Field Site

The Seine estuary is a meandering system subjected to a macrotidal regime (Fig. 1). The estuary is hyposynchronous with a double high tide during spring tide conditions (tidal range of 8 m) and synchronous during neap tide conditions (tidal range of 4 m; Guezennec 1999; Guezennec et al. 1999). The tidal range decreases from 8 m at the mouth to 2.5 m at the tidal limit during spring tides. The tidal propagation is stopped 160 km upstream from the mouth by the Poses lock and low tidal reflection was observed. Study sites in the estuary were determined using the kilometric point (kp) location system established for French estuaries (Table 1). The reference position kp0 is Pont Marie (Paris), and the upstream limit of the Seine estuary is located at kp202 (Fig. 1).

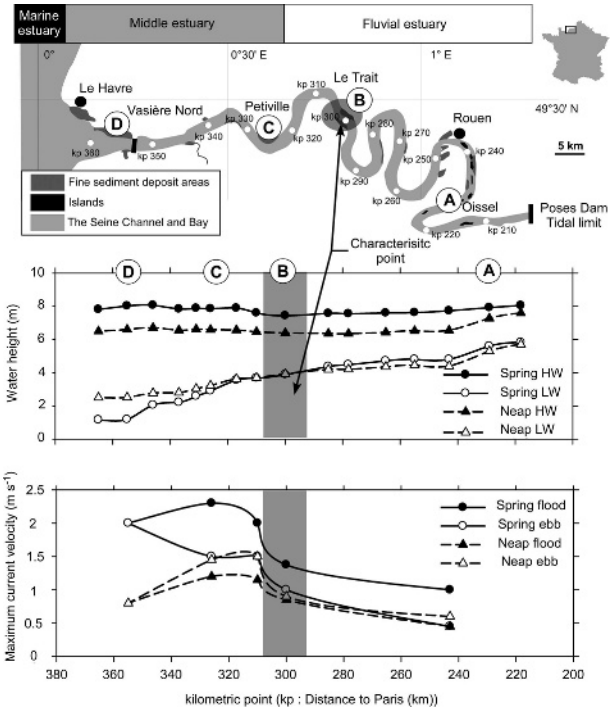

Fig. 1. The Seine estuary: hydrodynamic features and sites studied. Main channel current velocity values provided with permission from the Port Autonome de Rouen (from Guezennec 1999). Channel width exaggerated upstream kp 350 to clarify the figure.

Guezennec (1999) identified three compartments in the Seine estuary by considering salt intrusion into the estuary (Fig. 1). The upstream compartment corresponds to the tide-affected fluvial freshwater zone, which is limited upstream by the tidal limit and downstream by the salt intrusion limit located near Caudebec en Caux 70 km from the mouth (kp310). The mid compartment corresponds to an area with a high salinity gradient where a turbidity maximum is observed during low water discharge periods (Avoine 1981; Guezennec et al. 1999; Le Hir et al. 2001). The marine compartment is limited to the estuary mouth and corresponds to a low salinity gradient area. Observations from Guezennec (1999) regarding water levels at low tide in neap and spring conditions identified the presence of a characteristic point near Le Trait (kp308) where low tide water levels are constant over a semilunar cycle (Fig. 1).

Few current velocity measurements have been undertaken in the Seine estuary; specific areas were studied near Rouen and at the estuary mouth, mainly in the main navigation channel (data from the Port of Rouen Authorities in Guezennec 1999). This primary data set was supplemented by results

TABLE 1. Nomenclature.

Latin Symbols	
C_d	Drag coefficient
C_{TKE}	Best fit coefficient for K - τ_{TKE} conversion
E_1, E_2	Empirical coefficients for the calculation of critical erosion shear stress
h (m)	Water height
K	Turbulent kinetic energy ($m^2\ s^{-2}$)
kp (km)	Location reference for the Seine (kp0 is the Pont Marie, Paris)
u,v,w ($m\ s^{-1}$)	Instantaneous current velocity components following the coordinates E,N,Up
$\bar{U}$, $\bar{V}$, $\bar{W}$ ($m\ s^{-1}$)	Average current velocity components
u′, v′, w′ ($m\ s^{-1}$)	Fluctuating current velocity components
U(z) ($m\ s^{-1}$)	Mean horizontal current velocity
u* ($m\ s^{-1}$)	Friction velocity
(W%)	Water content
z (m)	Recording height above the bed
z_0 (mm)	Bed roughness length
Greek Symbols	
α_F, α_E	U-u* best fit coefficients for ebb and flood stages
κ	Von Karman constant
ρ ($kg\ m^{-3}$)	Water density
ρ_b ($kg\ m^{-3}$)	Sediment bulk density
ρs ($kg\ m^{-3}$)	Dry sediment mass
τ_{ce} ($N\ m^{-2}$)	Critical erosion shear stress
τ_{re} ($N\ m^{-2}$)	Reynolds shear stress
τ_{COV} ($N\ m^{-2}$)	Total shear stress obtained from the Reynolds shear stress
τ_{TKE} ($N\ m^{-2}$)	Turbulent kinetic energy shear stress
$\tau_{VISCOUS}$ ($N\ m^{-2}$)	Viscous shear stress
τ_{LP} ($N\ m^{-2}$)	Shear stress calculated from the LP method
ν ($m^2\ s^{-1}$)	Kinematic viscosity of water
ξ	Empirical constant for calculation of critical erosion shear stress

from validated numerical models (Brenon and Le Hir 1999). These results revealed longitudinal variations in flood and ebb currents as tides propagate into the estuary (Fig. 1; Brenon 1997). During spring tide and low water discharge conditions, the current velocity in the main channel is characterized by a strong flood current for a short period in the mouth (2 m s^{-1} current velocity for a 1-h period), a 4-h period with flood current velocities below 0.5 m s^{-1}, and a long constant ebb current velocity period with a current speed of 1 m s^{-1}. These maximal flood and ebb current velocities in the main channel as well as the flood:ebb current ratio first increase in the middle estuary (flood current velocity of 2.5 m s^{-1}) and then decrease upstream, with 1 m s^{-1} flood current velocity at the water surface measured near Le Trait (Fig. 1) and 0.5 m s^{-1} in Rouen 20 km downstream from Oissel (Guezennec 1999).

Current velocities were not homogenously distributed in cross sections due to the meandering morphology. Guezennec (1999) measured surface current velocity in the inner and outer parts of a meander in the Seine estuary 20 km downstream from Rouen. This author showed that maximum flood (respectively maximum ebb) current velocity in the outer part was 50% higher than in the inner part (30%). The maximum flood current velocity decreased from 1.0 m s^{-1} in the outer part to 0.6 m s^{-1} in the inner part, and maximum ebb currents decreased from 1.0 to 0.7 m s^{-1}. As a result, these lower hydrodynamic intensity zones are preferential areas for deposition of fine sediments.

In order to determine variability of shear stress intensity from the upstream tidal limit to the estuary mouth, stations typical of mudflats of these areas were chosen as sites for hydrodynamic measurements (Fig. 1). These stations are listed in order from the fluvial to the marine part of the estuary. The Oissel mudflat (A; kp230) is a typical fine sediment storage area for the undredged fluvial part of the estuary (Guezennec et al. 1999; Deloffre et al. 2005). Le Trait mudflat (B; kp300) is located downstream from Rouen, where the fluvial estuary is embanked and dredged, and near the characteristic point discussed by Guezennec et al. (1999). Petiville mudflat (C; kp325) is located in the turbidity maximum zone during low water discharge and is representative of the middle estuary. Stations A, B, and C are located in the center of the mudflat away from large natural or human structures that could perturb the river flow. These stations are located 2 m above the low water tide level, so they are subjected to comparable flood and ebb durations. They are not influenced by wind, but wave events caused by barges and sea vessels occur intermittently. The Vasière Nord (D; kp355) is the largest mudflat of the Seine estuary and is located at its mouth (Lesourd et al. 2003). This site differs from the others as it is separated from the main channel by a submersible dyke, and is crossed by large runnels. It is located 6 m above the low water tide level, and is consequently only flooded during slack water periods. The flood and ebb periods are shorter and tidal currents are assumed to be lower than those observed at the other stations. This mudflat was chosen because of its importance in terms of sediment storage capacity. Station D is mainly controlled by wind waves and swell (Lesourd et al. 2003; Deloffre et al. in press).

Measurements were made during successive tidal cycles at stations A, B, and C from May 3, 2004 to May 13, 2004, i.e., during spring and neap conditions. Spring tide corresponds to tidal amplitudes over 7.5 m at the mouth and neap tide to tidal amplitudes below 6.8 m. Spring and neap tide surveys were carried at station D on March 21, 2003 and March 31, 2003, respectively. Tidal amplitude for these two surveys was 8.05 and 7.5 m, respectively. Due to the altitude of station D, the water

height above the mudflat did not exceed 0.5 m for lower tidal range, which is the operational height limit for Acoustic Doppler Velocimeter (ADV) measurements. Throughout the surveys, river water discharge was lower than 400 $m^3 s^{-1}$, which is the mean annual water discharge of the Seine River.

Materials and Methods

Measurement of Current and Calculation of Bed Shear Stress

The recent development of new acoustic Doppler devices, such as Acoustic Doppler Current Profiler (ADCP) and ADVs, enables high frequency and high accuracy 3-dimensional current velocity measurements and consequently a good quality measurement of turbulence (Kawanisi and Yokosi 1997; Fugate and Friedrichs 2002; Nikora et al. 2002; Voulgaris and Meyers 2004; Simpson et al. 2005).

All stations were measured with a 6 MHz Nortek Vector Acoustic Doppler Velocimeter. Shear stress intensities in the water column reach the highest values close to the sediment-water interface (Simpson et al. 2005). Higher in the water column, the turbulent energy is partially dissipated and its intensity decreases. The ADV was consequently set up for near-bed measurements with the 0.8 cm^3 sampling cell located 7 cm above the bed. The apparatus was fixed on a rigid aluminium frame and directed perpendicularly towards the main channel axis to minimize frame-induced noise. This setup is particularly suitable for shear stress measurements as discussed in various studies (Kawanisi and Yokosi 1997; Kim et al. 2000; Nikora et al. 2002; Voulgaris and Meyers 2004). Velocity measurements were recorded in the East/North/Up coordinates, automatically compensating for possible movement of the instrument using data provided by the ADV internal compass. This minimizes errors due to ADV misalignment with the vertical. The horizontal East/North coordinates were changed to the streamward/crossward reference coordinates, u is then the alongshore velocity and v is the cross-shore velocity.

ADV enables measurement of the three components of current velocity with an accuracy of 0.5% of the measured velocity, 7 cm above the bed. Each component of the instantaneous velocity u,v,w can be separated into an averaged part $\bar{U}$, $\bar{V}$, $\bar{W}$ and a fluctuating part u′,v′,w′, such as: $u = \bar{U} + u'$ (v and w, respectively). The average time step was set to 1 min for calculations. Spectral analysis of the velocity components u, v, and w was performed and, throughout the experiments, noise disturbance was only observed on rare occasions. In the case of noisy measurements, the high frequency signal is filtered and removed.

The three mathematical formulations most used in the literature are described below.

The Near-bed Logarithmic Profile Method

Classical tank turbulence measurements are based on the logarithmic velocity profile method (LP), which uses the von Karman-Prandtl equation to estimate the friction velocity u*:

$$\frac{U(z)}{u*} = \frac{1}{\kappa}\log\left(\frac{z}{z_0}\right) \quad (1)$$

where U(z) is the mean current velocity at height z above bed, κ is the Von Karman constant, and z_0 is the bed roughness length. This method requires velocity measurements at various heights in the water column to reproduce and fit the current velocity log profile (Fugate and Friedrichs 2002). For studies requiring single point measurements, as was the case in the present study, correct estimation of the bed roughness value is needed. Recent studies revealed the complexity involved in estimating roughness value, with measurements ranging from 0.1 to 1 mm for muddy sediment (Voulgaris and Meyers 2004). Soulsby (1997) proposed values ranging from 0.2 mm for muddy sediments to 0.7 mm for mud-sand sediment. The Seine intertidal mudflats concerned here are mainly made of mud, and a bed roughness value of 0.2 mm was used. To compare methods used to calculate shear stress values, the friction velocity u* calculated from the LP method was transformed to the bottom shear stress τ_{LP} value by applying:

$$\tau_{LP} = \rho\, u*^2 \quad (2)$$

The Covariance Method

Calculating the total shear stress based on the covariance (COV) method requires both the Reynolds shear stress (τ_{Re}) and the viscous stress ($\tau_{VISCOUS}$; Stacey et al. 1999). Nikora et al. (2002) estimated $\tau_{VISCOUS}$ using the linear relationship expressing viscous stress as a function of the time-averaged current velocity and the distance z up to the bed:

$$\tau_{VISCIOUS} = \rho\, \nu \frac{\overline{du}}{dz} \cong \rho\, \nu \frac{|U(z)|}{z} \quad (3)$$

τ_{Re} was estimated using the classical relationship involving the two Reynolds components:

$$\tau_{Re} = -\rho\left(\overline{u'w'} + \overline{v'w'}\right) \quad (4)$$

(Soulsby 1983; Dyer et al. 2004; Voulgaris and Meyers 2004). Total shear stress (τ_{COV}) is estimated as: $\tau_{COV} = \tau_{Re} + \tau_{VISCOUS}$.

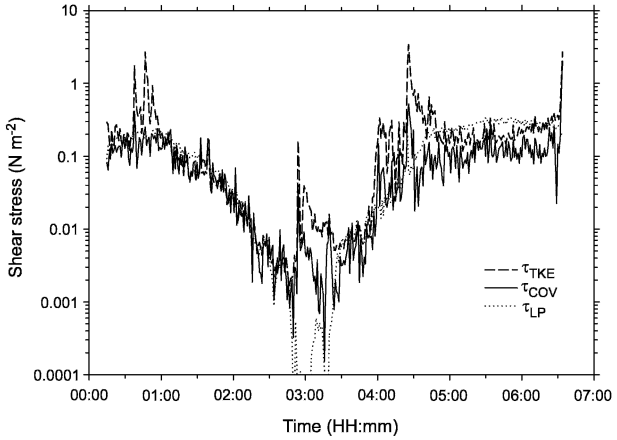

Fig. 2. Turbulent shear stress values calculated with three different methods: turbulent kinetic energy (TKE), logarithmic profile (LP), and covariance (COV). Case of a tidal survey at Le Trait (station B). The LP shear stress is calculated considering a bed roughness length value of 0.2 mm.

The Turbulent Kinetic Energy Method

The turbulent kinetic energy (TKE) method expresses the TKE shear stress (τ_{TKE}) proportionally to the turbulent kinetic energy K:

$$K = \frac{1}{2}\left(\overline{u'^2} + \overline{v'^2} + \overline{w'^2}\right) \quad (5)$$

$$\tau_{TKE} = \rho\, C_{TKE}\, K \quad (6)$$

C_{TKE} coefficient values ranging from 0.19 to 0.21 are commonly cited in the literature for near-bed measurements (Soulsby 1983; Kim et al. 2000). In our study, all measurements were made at the same height above the bottom, i.e., 7 cm above the bed, and an average constant value of 0.2 was used for the calculation of τ_{TKE}.

A typical data set recorded at Le Trait mudflat during neap tide is presented in Fig. 2 to compare the mathematical formulations used to calculate shear stress values. This comparison reveals that the three methods are well correlated. The LP shear stress values exceed τ_{COV} values during high current velocity periods for both flood and ebb periods. This could be due to the variability of the surface sediment properties, i.e., bed roughness length.

Discrepancies at Le Trait mudflat were observed during short events with high shear stress values ($\tau_{TKE} > 1$ N m^{-2}). These events were caused by waves generated by barges or sea vessels sailing the Seine estuary. The LP method is not sensitive to waves as it is based on mean current velocity measurements. The TKE method is highly influenced by waves because orbital velocities increase fluctuations in velocity (Soulsby and Humphery 1990).

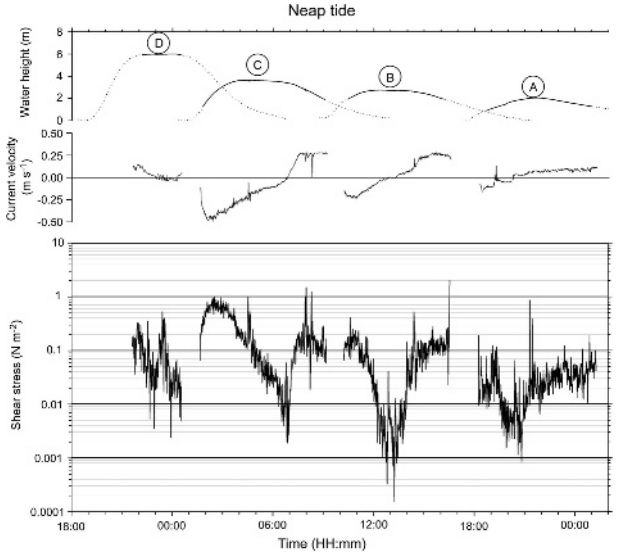

Fig. 3. Time series of water height, current velocity, and total shear stress (τ_{COV}) above the four intertidal mudflats in neap tide conditions. A) Oissel, B) Le Trait, C) Petiville, and D) Vasière Nord. Solid line symbolizes the flooded periods and the dotted line is the water height in the main channel.

Effects of wave events are beyond the scope of this study and will not be discussed further in this paper. Our interpretation and discussion of the results only focuses on periods not affected by wind waves or boat-induced waves, where the three methods are equivalent. τ_{COV} is used to represent shear stress values, clarifying our results.

Sediment Features

Sediment bulk density and grain-size distribution of each mudflat were measured during each tidal survey. Bed sediments were collected just after mudflat emersion and measurements were made in the laboratory. Grain-size distributions were obtained with a Beckman laser Coulter LS 230 measuring a size spectrum from 0.04 to 2,000 μm. Bulk density was obtained from water content measurements (W%):

$$\rho_b = \rho + \left(\frac{\rho_s - \rho}{\rho_s}\right)\left(\frac{\rho}{\frac{W\%}{100} + \frac{\rho}{\rho_s}}\right) \quad (7)$$

where W% is the ratio between the water mass and the dry sediment mass.

Results

Neap Tide

Figure 3 presents the general hydrological conditions on the mudflats studied along the Seine estuary in neap tide conditions. The water height

zero reference was set locally at the low slack water level for each site. The tidal range during neap tide is 6 m at the mouth, decreases upstream to 4 m at station C, and reaches 2 m close to the dynamic tidal limit at station A. Maximum water height at station D did not exceed 1.5 m due to the altitude of the mudflat. Similar to water height, the maximum current velocity measured above the intertidal mudflats decreases from the mouth to the fluvial part of the estuary from 0.5 to 0.2 m s^{-1}, respectively.

The first station located in the upstream fluvial part was ebb dominated. The flood period in station A was short and of low intensity with current velocity values lower than 0.2 m s^{-1}. Flood-ebb current reversal occurred 2 h before high water, and ebb currents slowly rose to reach a maximum value of 0.2 m s^{-1}.

The hydrodynamics at station B was flood-ebb balanced, with symmetrical behavior before and after high water. The maximum current velocity was 0.25 m s^{-1} at the beginning of the flood period and at the end of the ebb period, and current velocity inversion occurred during the high slack water period.

Stations C and D were flood dominated. Flood currents at station C rapidly reached the maximum values of 0.4 m s^{-1} half an hour after mudflat immersion, and decreased slightly until flood-ebb current reversal 2 h after high water. Ebb currents increased rapidly to reach a mean velocity value of 0.3 m s^{-1}. Station D is located on the Vasière Nord mudflat, 4 m higher than the other stations and despite the large tidal range at the estuary mouth, only the end of the flood period, slack water, and the onset of the ebb period were recorded, i.e., the periods of lower energy during a tidal cycle. The mudflat was characterized by low water height (below 60 cm) and low current velocities (below 0.2 m s^{-1}) in neap tide conditions.

Spring Tide

During the spring tide conditions, a tidal range of 8 m was observed at the estuary mouth, this range decreased slightly to reach 3 m at station A close to the tidal limit (Fig. 4). The tidal wave propagates into the estuary with a pronounced asymmetric shape that increases from the estuary mouth to the upstream boundary. A double high water slack was observed at stations C and D. The hydrodynamic features in spring tide conditions were similar to those observed during neap tides at the downstream stations B, C, and D, with higher current velocities up to 1 m s^{-1} at station C. Differences were observed at station A where the current reversal period corresponded to the high slack water period and flood and ebb periods followed a similar pattern with maximum current speed of 0.2 m s^{-1} and equal ebb-flood periods.

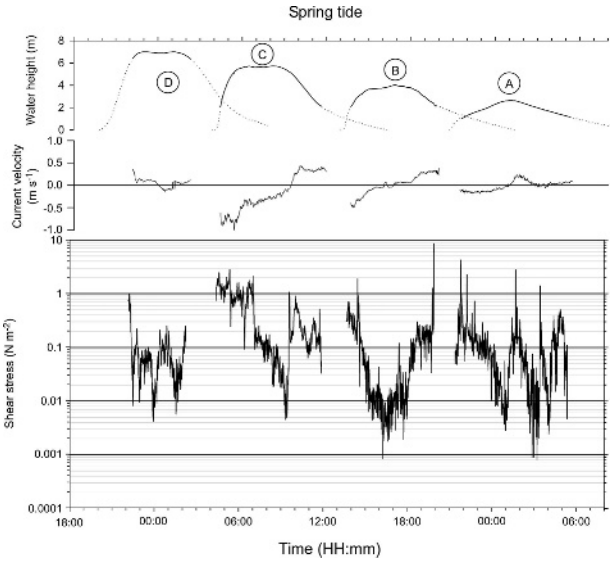

Fig. 4. Time series of water height, current velocity, and total shear stress (τ_{COV}) above the four intertidal mudflats in spring tide conditions. A) Oissel, B) Le Trait, C) Petiville, and D) Vasière Nord. Solid line symbolizes the flooded periods and the dotted line is the water height in the main channel.

Shear Stress Measurements

Shear stress variations for neap and spring tides conditions are presented in Figs. 3 and 4. τ_{COV} decreased from the estuary mouth to the fluvial part, with maximum values of 0.8, 0.15, and 0.05 N m^{-2} for stations C, B, and A during neap tide conditions and 1, 0.4, and 0.2 N m^{-2} during spring tide conditions, respectively.

Shear stress variations during a tidal cycle for both neap and spring tides were similar for stations B and C. Large shear stress values were observed on mudflats during flood and ebb periods, and values less than 0.01 N m^{-2} were observed during high slack water periods. The occurrence of the maximum shear stress value above the intertidal mudflats during the tidal cycle depends on the location of the station in the estuary and on the moment in time in the semilunar cycle. The highest τ_{COV} were observed during flood periods in both neap and spring tide conditions at station C (τ_{COV} values of 0.8 and 1 N m^{-2}, respectively) and during spring tide conditions at station B (τ_{COV} value of 0.4 N m^{-2}). Shear stress values during neap tides at station B were similar for both flood and ebb periods, with a τ_{COV} value of 0.15 N m^{-2}. During neap tides, τ_{COV} values below 0.05 N m^{-2} were measured at station A. During spring tide conditions, τ_{COV} reached values exceeding 0.1 N m^{-2} during the flood period, the high slack water period, and the ebb period.

Due to the higher altitude of the mudflat, station D was never subjected to the most energetic flood and ebb conditions and did not display noticeable shear stress during neap and spring tides. The station D mudflat experienced τ_{COV} values that were consistently greater than 0.05 N m^{-2} while current velocity values were less than 0.1 m s^{-1}. These shear stress values can be attributed to periods of wind or waves of small amplitude (<0.05 m) but which nevertheless had a marked influence on the bottom shear stress due to the low water height (<0.6 m).

Discussion

Comparative Methods for Calculation of Shear Stress

According to Kim et al. (2000), TKE, COV, and LP methods present similar values (Fig. 2). The combined use of these three methods of calculation can be a useful way to evaluate the individual effects of the parameters that control turbulent processes, i.e., tidal currents and waves. The LP method, which is based on mean current velocities, is useful to determine tidally-induced shear stress because high frequency variations are integrated in the time averaging operation. The LP method is optimal when current velocity profiles are recorded as it allows both accurate calculations of bed roughness length and shear stress values. This method can also be used when current velocity profiles are not available but in this case requires a priori estimation of the bed roughness length value. This estimation generates serious errors in the friction velocity calculations (Fig. 2). TKE and COV methods operate from similar inputs, i.e., the fluctuating part of the current velocity, but with the TKE method, shear stress values are calculated from the turbulent kinetic energy K by using Eq. 6. τ_{TKE} then depends on the choice of the C_{TKE}, which ranges from 0.19 (Soulsby 1983; Dyer et al. 2004) to 0.21 (Kim et al. 2000). With tidal flows, COV and TKE methods are theoretically equivalent, and τ_{COV} and τ_{TKE} can be compared as:

$$\tau_{COV} = \tau_{TKE} = \rho\, C_{TKE}\, K \qquad (8)$$

The comparison of the combined results of spring and neap surveys is presented in Fig. 5; a linear regression was used to estimate C_{TKE}. Values were well correlated ($r > 0.95$) with the best fit C_{TKE} value of 0.19 (Fig. 5), in agreement with the value proposed by Soulsby (1983).

Relationships between Tidal Currents and Friction Velocity

Correlations between observations of current velocity and turbulence shear stress measurements are obvious if both friction velocities calculated from the τ_{COV} and the time-averaged current velocities are plotted, after truncating the wave events (Fig. 6). Considering the flow as fully turbulent, the friction velocity u* is calculated as a function of the local shear stress at the height z and empirically corrected from the water height variations:

$$u* = \sqrt{\frac{\tau_{COV}}{\rho(1 - z/h)}} \qquad (9)$$

(Voulgaris and Trowbridge 1998; Stacey et al. 1999; Voulgaris and Meyers 2004).

Linear regression fits are based on the following formulation: $u* = \alpha(U + \beta)$. The constant in the regression line is always smaller than 0.001, which validates the logarithmic form of the flow and data consistency (Collins et al. 1998). Flood and ebb components are fitted separately (α_F and α_E correspond respectively to flood and ebb periods) in order to examine possible changes in the bed sediment properties with respect to flood and ebb periods as found by Collins et al. (1998) and Voulgaris and Meyers (2004). These coefficients are related to the drag coefficient values measured close to the bed by applying the formulation: $C_d = \alpha^2$. Calculating best-fit linear relationships between current velocity and friction velocities is equivalent to estimating the bed roughness by applying the LP method used for bed shear stress calculations (Eq. 1). This equation can be transformed to express u* as a function of the mean value of the time series of current velocity values U(z), and becomes (Collins et al. 1998):

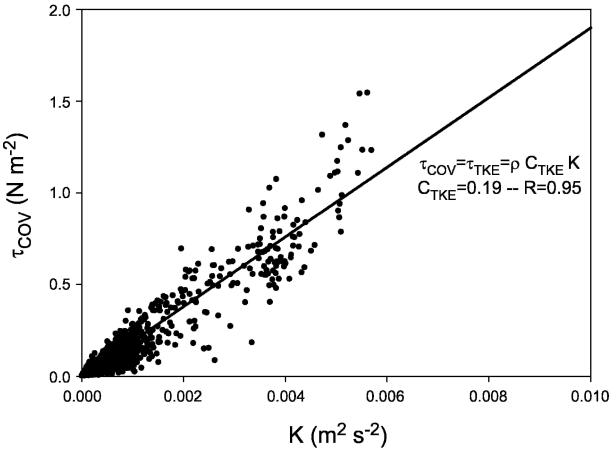

Fig. 5. Relationship between the turbulent kinetic energy (K) and the total shear stress (τ_{COV}) values. The solid line shows the best fit (linear least squares regression analysis) of τ_{COV} values regarding K ones. The constant $C_{TKE} = 0.19$ value is deduced from this linear fit.

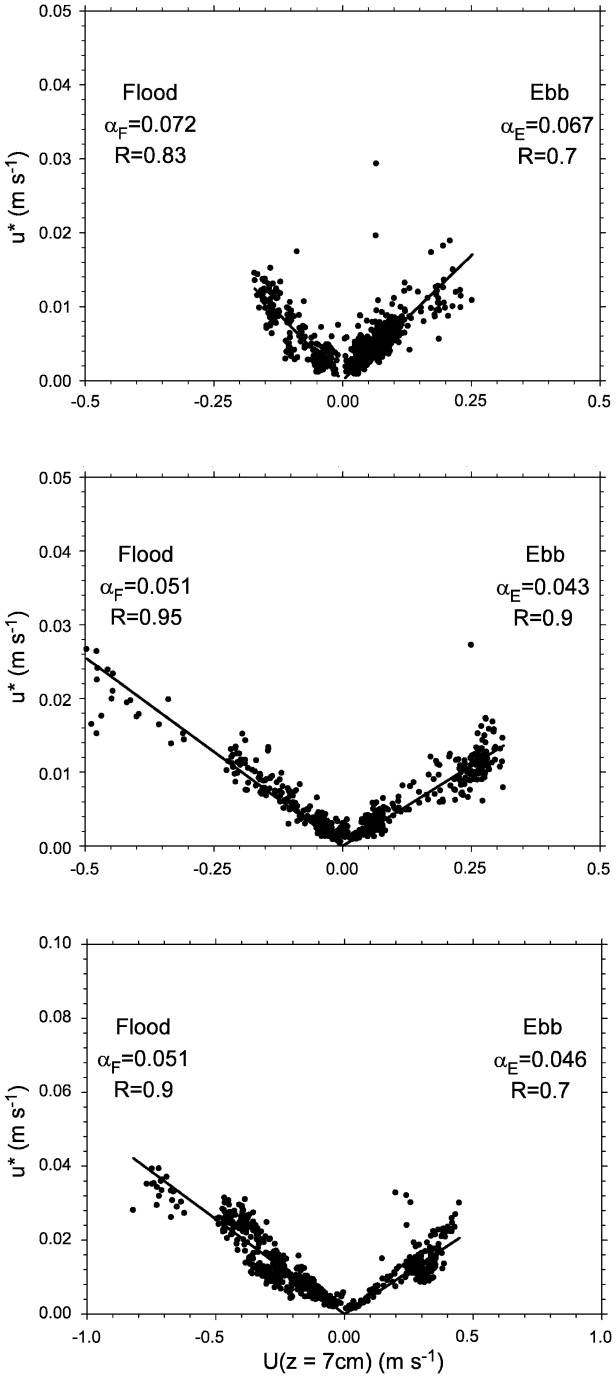

Fig. 6. Friction velocity as a function of the mean current velocity: linear relationship fits.

$$u* = \frac{\kappa}{\ln(z/z_0)} U \qquad (10)$$

The best-fit regression coefficient α is related to the bed roughness value, assuming that the sampling height z is known (in the present study, z = 7 cm; Table 2). In this study, the bed roughness is considered to be only skin roughness and is associated with sediment grain-size characteristics. In our study, topographic variations in bedform that also contribute to the bed roughness length were not considered, as the deployment station was located in the flattest area of the mudflats far from runnels and channels.

Current velocities and friction velocities values are well correlated (Fig. 6 and Table 2), and a consistent feature was observed at the three stations with higher best-fit constant values during flood periods, and higher drag coefficient and bed roughness values. The bed roughness length decreased from 0.34 mm during the flood stage to 0.18 mm during the ebb stage at station A and from 0.03 to 0.01 mm at stations B and C. These observations could be due to a change in sediment properties during the tidal cycle, which, in turn, could be due to finer grained sediment or biological activity (Voulgaris and Meyers 2004). Averaged bed roughness length values were calculated to 0.02 mm for stations B and C and 0.26 mm for station A. These variations in length could be due to specific sediment properties at stations A, B, and C. Bed roughness length values were then compared with bed sediment features (Table 3). Bed sediments at stations B and C were mostly muddy, and the calculated bed roughness length values are close to the median value (30 μm) of the sediment particle size distribution (Table 3). The bed roughness length value at station A is three times higher than the median size of 77 μm. Sediment at station A is a mixture of sand and mud, with mode values of 120 and 20 μm, respectively. Mitchener and Torfs (1996) showed that values for bed roughness length are high for mixed bed sediments, which could explain the high bed roughness length values found here. These results are in agreement with the recent work of Voulgaris and Meyers (2004) who estimated bed roughness length values ranging from 0.026 to 0.1 mm for silt sediments with an occasional sand fraction. They are lower than those proposed by Soulsby (1997) i.e., 0.2 mm for mud and 0.7 mm for a sand-mud mixture. Unlike the Nikuradse formula that gives the bed roughness length as 1/12 fold the median size of sand grains, the linear relationship between particle-size distribution and bed roughness length for muddy or sand-mud sediments for mudflats with no topographic effect is: $z_0 \approx D_{50}$ for muddy sediments and $z_0 \approx 3\ D_{50}$ for mud-sand mixtures.

The 0.2 mm bed roughness length value was initially chosen to determine shear stress values by the LP method, which explains the fact that LP shear stress values exceed the τ_{COV} ones during maximal ebb and flood current velocities. The use of a single constant value for bed roughness length

TABLE 2. Summary of drag coefficient, bed roughness, and best-fit constant values at Oissel (station A), Le Trait (station B), and Petiville (station C) calculated during flood and ebb stages.

	Flood			Ebb		
Site	α	C_d ($\times 10^{-3}$)	z_0 (mm)	α	C_d ($\times 10^{-3}$)	z_0 (mm)
A	0.072	5.6	0.34	0.067	4.5	0.18
B	0.051	2.6	0.027	0.043	1.8	0.006
C	0.051	2.8	0.027	0.046	2.1	0.012

during tidal cycles introduces uncertainty in the estimation of bed shear stress. To give an example, for a water current velocity of 0.5 m s^{-1}, a change in the bed roughness value from 0.34 to 0.18 mm, as observed at station A, causes a reduction in bottom shear stress from 1.41 to 1.12 N m^{-2}. This generates an error of 20% in the estimation of τ_{LP}. Careful use of the bed roughness length is required in estuarine systems studies where successive periods of sedimentation and erosion induce a continuous change in the nature of sediment.

Effect of Tidally-induced Turbulence on Sediment Dynamics

Based on the present set of data, the near-bed tidally-induced shear stress can be calculated along the macrotidal Seine estuary. Variations in shear stress have a powerful influence on estuarine processes and typical sediment dynamics by controlling bank erosion and sediment resuspension and deposition. Recent studies reported the development of many in situ devices (Tolhurst et al. 2000) or laboratory devices (Mitchener and Torfs 1996) to measure critical erosion shear stress (τ_{ce}). Field and laboratory experiments on various mixed-sediment samples provided a large data set that can be used to propose a simple empirical relationship between sediment properties and erosion critical shear stress values. No τ_{ce} measurements were made during the present study, and consequently τ_{ce} estimations were made using different empirical relationships given in the literature linking τ_{ce} and bed bulk density ρ_b.

Mitchener and Torfs (1996) proposed calculating τ_{ce} as a power function of ρ_b

$$\tau_{ce} = E_1(\rho_b - 1{,}000)^{E_2} \qquad (11)$$

with $E_1 = 0.015$ and $E_2 = 0.73$. This formulation has been validated for artificial sand-mud mixed sediment with bulk density values ranging from 1,000 to 1,800 kg m^{-3}. The results obtained from natural undisturbed sediment with properties close to those observed on the mudflats studied here were one order of magnitude lower than the artificial sediments and varied with the mud : sand ratio. To give an example, τ_{ce} measured for sediments similar to those in the present study with bulk density values varying from 1,200 to 1,400 kg m^{-3} range from 0.05 to 0.7 N m^{-2} for muddy sediment containing 0% and 20% of sand, respectively, and the associated calculated τ_{ce} is 0.95 N m^{-2} ($\rho_b \sim$ 1,300 kg m^{-3}). The given relationship overestimates critical erosion shear stress values.

Mehta (1988) found the critical erosion shear stress to be a function of the bulk density ρ_b and a ξ coefficient:

$$\tau_{ce} = \xi\left(\frac{\rho_b - 1{,}000}{1{,}000}\right) \qquad (12)$$

ξ is generally estimated to be 1 for cohesive sediments, but this coefficient may be one order of magnitude higher with a sediment with 18% sand content. The calculated τ_{ce} is 0.3 N m^{-2} for a bulk density value of 1,300 kg m^3. These τ_{ce} values are close to those measured by Tolhurst et al. (2000) on similar sediments. These two relationships can be used to estimate τ_{ce} values. All the controlling parameters such as grain-size distribution and benthic biological activity, which are known to stabilize bed sediments (Mitchener and Torfs 1996; Riethmuller et al. 2000; Tolhurst et al. 2000; Droppo et al. 2001), are not taken into account. Table 3 summarizes bed sediment features and a range of values of τ_{ce} values calculated with the two methods presented above for the four mudflats investigated in the Seine estuary. Seine mudflat

TABLE 3. Bed sediment properties at the four mudflats studied.

Station	Site	Bed Concentration (g l^{-1})	Bulk Density (g l^{-1})	% Mud	% Sand	Calculated Critical Erosion Shear Stress (Range in N m^{-2})
A	Oissel	678.5	1,422.4	73.5	26.5	0.42–1.2
B	Le Trait	476.5	1,296.7	82.0	18.0	0.3–1.0
C	Petiville	431.2	1,268.5	84.0	16.0	0.25–0.9
D	Vasière Nord (NT)	578.9	1,360.4	—	—	0.36–1.1
D	Vasière Nord (ST)	389.5	1,242.5	—	—	0.24–0.8

sediments are mixed mud and sand with a higher sand content (>25%) and a higher bulk density (1,420 kg m^{-3}) at the upstream station A. Consequently bed sediment at station A is the most stabilized, with τ_{ce} values ranging from 0.4 to 1.2 N m^{-2}. Two critical erosion shear stress intervals are given for station D because a deposition period occurred between the spring and neap surveys. Surface sediment properties varied during these periods and τ_{ce} values ranged from 0.36 to 1.1 N m^{-2} and from 0.24 to 0.8 N m^{-2} before and after deposition, respectively (Table 3). These results are close to the rheological values obtained by Lesourd (2000) on mud samples collected at the mouth of the Seine estuary and used for consolidation experiments. τ_{ce} values estimated by this author ranged from 0.4 to 0.8 N m^{-2}, with a rapid increase in τ_{ce} from 30% to 200% 1 h after the onset of the experiment. These calculated intervals of critical erosion shear stress were compared with the calculated total shear stress (τ_{COV}) for each site during neap and spring conditions. This comparison reveals that the tidally-induced shear stress never exceeds the critical erosion shear stress values at stations A and D, whatever the spring or neap conditions. At station B and only during the early flood stage on spring tide, τ_{COV} values are higher than the lowest calculated τ_{ce} values. Only station C is seen to be controlled by the tidal currents, mostly during the flood period and whatever the hydrodynamics conditions. These results provide a first approach to understanding how tidal currents control the process of mudflat erosion. These results are based on simple calculations where τ_{ce} is only a function of the bulk density. The ADV is operational as soon as sensors are flooded, when the water height above the mudflat exceeds 20 cm, so it is not possible to make measurements at the critical periods of flood and ebb, when the water just starts to come in and to go out. This means that maximal shear stress values could be underestimated. Both shear stress and τ_{ce} field measurements are now required to confirm the role played by tidal flows in estuarine mudflat dynamics.

Hydrodynamic Compartments within the Macrotidal Seine Estuary

The results obtained in this study are in good agreement with turbulence measurements recently made in macrotidal estuarine systems (Kawanisi and Yokosi 1997; Dyer et al. 2004; Voulgaris and Meyers 2004). Some of these sampling stations were located in channels where shear stress values are the highest, while in this present study, the instruments were positioned on several intertidal mudflats. Most of these authors' experiments were carried at a single point in an estuary cross section and cannot describe the spatial variability of the hydrodynamic features.

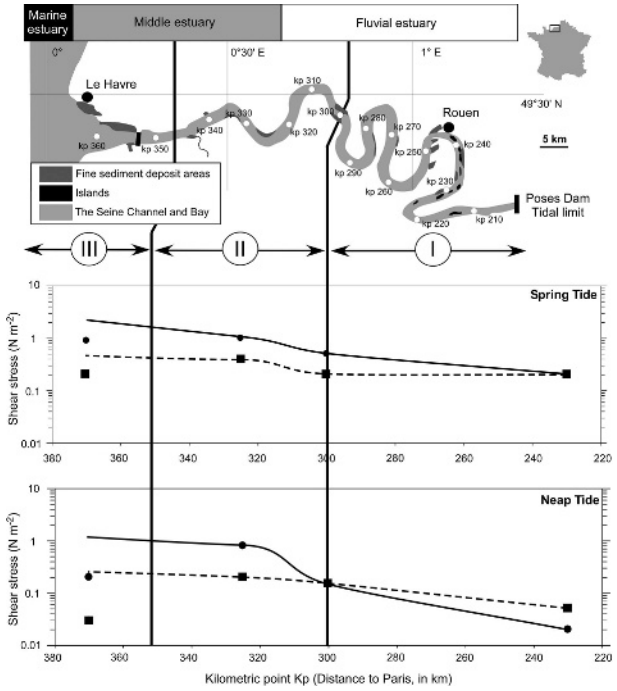

Fig. 7. Maximum tidally-induced shear stress values on intertidal mudflats along the Seine estuary during flood (black dots) and ebb stages (black squares), during neap and spring tide conditions. The dashed line represents the schematic evolution of the bed shear stress for mudflats located 2 m above the low water height. Dark lines symbolizes the flood phase and grey lines the ebb phase.

Our results provide support for dividing the Seine estuary into three specific compartments according to the conceptual model proposed by Dalrymple et al. (1992) for meandering tide-dominated estuaries that we modified to consider only intertidal environments (Fig. 7). Two main compartments can be proposed. The first compartment (I) is limited upstream by the dynamic tidal limit and downstream at the characteristic point located near station B. This compartment is ebb-dominated with averaged calculated shear stress values lower than 0.3 N m^{-2} that do not allow sediment resuspension. The second compartment (II) is limited upstream at the characteristic point and downstream at the marine limit of the estuary. This compartment is flood dominated and the tidally-induced shear stress values reach of 1 N m^{-2} close to the τ_{ce}. Intertidal mudflats at the estuary mouth are located 6 m above the low water level and do not present comparable shear stress values. Station D experiences low tidal current velocities and low tidally-induced shear stress values (<0.1 N m^{-2}). Previous works carried out at the mouth of the estuary led to

a proposal for a third compartment in this area, related to intertidal mudflats, where wind effects are predominant (Silva Jacinto 2002; Lesourd et al. 2003; Deloffre et al. in press).

Acknowledgments

Funding for this study was partly provided by the European INTERREG III RIMEW program and the Seine Aval Program. Three anonymous reviewers are acknowledged for their helpful comments. We would like to thank Mrs. Daphne Goodfellow for her helpful review. Jonathan Taylor and Romaric Verney were funded through two grants provided by the Regional Council of Haute Normandie (France).

Literature Cited

Avoine, J. 1981. Estuaire de la Seine: Sédiments et dynamique sédimentaire, Université de Caen, Normandy, France.

Black, K. S. 1998. Suspended sediment dynamics and bed erosion in the high shore mudflat region of the Humber Estuary, U.K. *Marine Pollution Bulletin* 37:122–133.

Brenon, I. 1997. Modélisation de la dynamique des sédiments fins dans l'estuaire de Seine, Thèse de 3ème cycle, Université de Bretagne Occidentale, Brest, France.

Brenon, I. and P. Le Hir. 1999. Modelling the turbidity maximum in the Seine estuary (France): Identification of formation processes. *Estuarine Coastal and Shelf Science* 49:525–544.

Collins, M. B., X. Ke, and S. Gao. 1998. Tidally-induced flow structure over intertidal flats. *Estuarine Coastal and Shelf Science* 46:233–250.

Dalrymple, R. W., B. A. Zaitlin, and R. Boyd. 1992. Estuarine facies models: Conceptual basis and stratiographic implications. *Journal of Sedimentary Petrology* 62:1130–1146.

Deloffre, J., R. Lafite, P. Lesueur, S. Lesourd, R. Verney, and L. Guezennec. 2005. Sedimentary processes on an intertidal mudflat in the upper macrotidal Seine estuary, France. *Estuarine, Coastal and Shelf Science* 64:710–720.

Deloffre, J., R. Lafite, P. Lesueur, R. Verney, S. Lesourd, A. Cuvilliez, and J. A. Taylor. in press. Controlling factors of rhythmic sedimentation processes on an intertidal estuarine mudflat—Role of the maximum turbidity zone in the macrotidal Seine estuary, France. *Marine Geology*.

Droppo, I. G., Y. L. Lau, and C. Mitchell. 2001. The effect of depositional history on contaminated bed sediment stability. *The Science of the Total Environment* 266:7–13.

Dyer, K. R. 1994. Estuarine sediment transport and deposition, p. 193–217. *In* K. Pye (ed.), Sediment Transport and Depositional Processes. Blackwell Scientific Publications, Oxford, U.K.

Dyer, K. R., M. C. Christie, N. Feates, M. J. Fennessy, M. Pejrup, and W. Van der Lee.. 2000. An investigation into processes influencing the morphodynamics of an intertidal mudflat, the Dollard Estuary, The Netherlands: I. Hydrodynamics and suspended sediment. *Estuarine Coastal and Shelf Science* 50:607–625.

Dyer, K. R., M. C. Christie, and A. J. Manning. 2004. The effects of suspended sediment on turbulence within an estuarine turbidity maximum. *Estuarine Coastal and Shelf Science* 59:237–248.

Eisma, D. 1993. Suspended Matter in the Aquatic Environment. Springer-Verlag, Berlin, Germany.

Eisma, D. 1996. Flocculation and deflocculation of suspended matter in estuaries. *Netherlands Journal of Sea Research* 20:183–199.

Fugate, D. C. and C. T. Friedrichs. 2002. Determining concentration and fall velocity of estuarine particle populations using ADV, OBS, and LISST. *Continental Shelf Research* 22:1867–1886.

Guezennec, L. 1999. Hydrdynamique et transport en suspension du matériel particulaire fin dans la zone fluviale d'un estuaire macrotidal: L'exemple de l'estuaire de la Seine (France), Thèse de 3ème cycle, Université de Rouen, Mont-Saint-Aignan, France.

Guezennec, L., R. Lafite, J. P. Dupont, R. Meyer, and D. Boust. 1999. Hydrodynamics of suspended particulate matter in the tidal freshwater zone of a macrotidal estuary (the Seine estuary, France). *Estuaries* 22:717–727.

Kawanisi, K. and S. Yokosi. 1997. Characteristics of suspended sediment and turbulence in a tidal boundary layer. *Continental Shelf Research* 17:859–875.

Kim, S.-C., C. T. Friedrichs, J. P.-Y. Maa, and L. D. Wright. 2000. Estimating bottom stress in tidal boundary layer from acoustic doppler velocimeter data. *Journal of Hydraulic Engineering* 126: 399–406.

Le Hir, P., A. Ficht, R. Silva Jacinto, P. Lesueur, J.-P. Dupont, R. Lafite, I. Brenon, B. Thouvenin, and P. Cugier. 2001. Fine sediment transport and accumulations at the mouth of the Seine estuary (France). *Estuaries* 24:950–963.

Le Hir, P., W. Roberts, O. Cazaillet, M. C. Christie, P. Bassoullet, and C. Bacher. 2000. Characterization of intertidal flat hydrodynamics. *Continental Shelf Research* 20:1433–1459.

Lesourd, S. 2000. Processus d'envasement d'un estuaire macrotidal: Zoom temporel du siècle à l'heure; application à l'estuaire de la Seine, Thèse de 3ème cycle, Université de Caen, Normandy, France.

Lesourd, S., P. Lesueur, J. C. Brun-Cottan, S. Garnaud, and N. Poupinet. 2003. Seasonal variations in the characteristics of superficial sediments in a macrotidal estuary (the Seine inlet, France). *Estuarine Coastal and Shelf Science* 58:3–16.

Maa, J. P.-Y., L. Sanford, and J. Halka. 1998. Sediment resuspension characteristics in Baltimore Harbour, Maryland. *Marine Geology* 146:137–145.

Manning, A. J. and K. R. Dyer. 1999. A laboratory examination of floc characteristics with regard to turbulent shearing. *Marine Geology* 160:147–170.

Mehta, A. J. 1988. Laboratory studies on cohesive sediment deposition and erosion, p. 427–445. *In* J. Dronkers and W. van Leussen (eds.), Physical Processes in Estuaries. Springer-Verlag, Berlin, Germany.

Mikes, D., R. Verney, R. Lafite, and M. Belorgey. 2004. Controlling factors in estuarine flocculation processes: Experimental results with material from the Seine estuary, northwestern France. *Journal of Coastal Research* SI 41:82–89.

Mitchener, H. and H. Torfs. 1996. Erosion of mud/sand mixtures. *Coastal Engineering* 29:1–25.

Nikora, V., D. G. Goring, and A. Ross. 2002. The structure and dynamics of the thin near-bed layer in a complex marine environment: A case study in Beatrix Bay, New Zealand. *Estuarine Coastal and Shelf Science* 54:915–926.

Riethmuller, R., M. Heineke, H. Kuhl, and R. Keuker-Rugiger. 2000. Chlorophyll *a* concentration as an index of sediment surface stabilisation by macrophytobenthos? *Continental Shelf Research* 20:1351–1372.

Sanford, L. P. and J. P.-Y. Maa. 2001. A unified erosion formulation for fine sediments. *Marine Geology* 179:9–23.

Silva Jacinto, R. 2002. Action des vagues sur les estrans et vasières. Application à l'estuaire de Seine, Thèse de 3ème cycle, Université de Rouen, Mont-Saint-Aignan, France.

Simpson, J. H., E. Williams, L. H. Brasseur, and J. M. Brubaker. 2005. The impact of tidal straining on the cycle of turbulence in a partially stratified estuary. *Continental Shelf Research* 25:51–64.

Soulsby, R. L. 1983. The bottom boundary layer of shelf seas, p. 189–266. *In* B. Johns (ed.), Physical Oceanography of Coastal and Shelf Seas. Elsevier, Amsterdam, The Netherlands.

Soulsby, R. L. 1997. Dynamics of Marine Sands. A Manual for Practical Applications. T. Telford, London, U.K.

Soulsby, R. L. and J. D. Humphery. 1990. Field observations of wave-current interaction at the sea bed, p. 413–428. *In* A.

Torum and O. T. Gudmestad (eds.), Water Wave Kinematics. Kluwer Academic Publishers, Dordrecht, The Netherlands.

STACEY, M. T., S. G. MONISMITH, AND J. R. BURAU. 1999. Measurements of Reynolds stress profiles in unstratified tidal flow. *Journal of Geophysical Research* 104:10933–10949.

TOLHURST, T. J., K. S. BLACK, D. M. PATERSON, H. J. MITCHENER, G. R. TERMAAT, AND S. A. SHAYLER. 2000. A comparison and measurement standardisation of four in situ devices for determining the erosion shear stress of intertidal sediments. *Continental Shelf Research* 20:1397–1418.

TOLHURST, T. J., R. RIETHMULLER, AND D. M. PATERSON. 2000. In situ versus laboratory analysis of sediment stability from intertidal mudflats. *Continental Shelf Research* 20:1317–1334.

UNCLES, R. J., A. E. EASTON, M. L. GRIFFITHS, C. K. HARRIS, R. J. M. HOWLAND, R. S. KING, A. W. MORRIS, AND D. H. PLUMMER. 1998. Seasonality of the turbidity maximum in the Humber-Ouse Estuary, U.K. *Marine Pollution Bulletin* 37:206–215.

UNCLES, R. J., J. A. STEPHENS, AND R. E. SMITH. 2002. The dependence of estuarine turbidity on tidal intrusion length, tidal range and residence time. *Continental Shelf Research* 22: 1835–1856.

VAN LEUSSEN, W. 1994. Estuarine Macroflocs: Their Role in Fine Grained Sediment Transport, University of Utrecht, Utrecht, The Netherlands.

VOULGARIS, G. AND S. T. MEYERS. 2004. Temporal variability of hydrodynamics, sediment concentration and sediment settling velocity in a tidal creek. *Continental Shelf Research* 24:1659–1683.

VOULGARIS, G. AND J. H. TROWBRIDGE. 1998. Evaluation of the acoustic doppler velocimeter (ADV) for turbulence measurements. *Journal of Atmospheric and Oceanic Technology* 15:272–289.

Received, June 10, 2005
Revised, March 8, 2006
Accepted, April 3, 2006